

Drag Reduction and Secondary-Flow Occurrence by Square Biplane Grid

Yoshino Tachimoto, Mitsuo Iwamoto, Hidemi Yamada

Department of Mechanical and Energy Systems Engineering, Oita University, Oita, Japan

Email: yamada@oita-u.ac.jp

How to cite this paper: Tachimoto, Y., Iwamoto, M. and Yamada, H. (2018) Drag Reduction and Secondary-Flow Occurrence by Square Biplane Grid. *Open Journal of Fluid Dynamics*, 8, 78-85.

<https://doi.org/10.4236/ojfd.2018.81007>

Received: February 15, 2018

Accepted: March 26, 2018

Published: March 29, 2018

Copyright © 2018 by authors and Scientific Research Publishing Inc.

This work is licensed under the Creative Commons Attribution International License (CC BY 4.0).

<http://creativecommons.org/licenses/by/4.0/>



Open Access

Abstract

In this paper, the characteristics of the three-dimensional flow field around the circular cylinder members forming a square biplane grid were experimentally investigated by using a wind tunnel and a water tunnel. In the wind tunnel testing, the span wise and circumference pressure distributions of surface on the circular cylinder were measured on the center mesh members formed by biplane grid in detail. Local drag coefficient was calculated from the surface pressure distributions. In addition, the flow visualization was performed in the water tunnel. As a result, it was suggested that the flow penetrating the contact region produced secondary-flow behind the biplane grid. Accordingly, the drag reduction would be caused by the presence of the secondary-flow.

Keywords

Biplane Grid, Circular Cylinders, Surface Pressure Distribution, Drag Coefficient, Flow Visualization

1. Introduction

There are two types of square lattice structures to control various industrial flow fields, biplane grid and woven screen. In particular, the square biplane grid which consists of many cylinders arrayed at right angles is often used to make turbulence. The turbulent characteristics downstream from the biplane grid have been examined in detail [1]. In addition, the heat transfer promotion may be expected in a new heat exchanger. Accordingly, it is important to reveal the flow characteristics around circular cylinders forming a biplane grid. Shiozaki *et al.* investigated drag coefficient and velocity distribution behind biplane grids and woven screens at a range of low Reynolds number ($Re = 1 - 300$) by numerical simulation [2]. Moreover, much research about grid turbulence has been per-

formed [3] [4] [5] [6], and the drag of woven screens which is similar to biplane grids has been studied [7]. However, the flow phenomenon around the circular cylinder forming a square lattice structure is not directly revealed. It is reported from the previous results of the crossed circular cylinders that the flow over the separation area on the upstream cylinder penetrates the vicinity of the contact point between upstream and downstream cylinders [8] [9]. Accordingly, it is supposed that the three-dimensional flow, which is similar to the crossed circular cylinders, is made in the cross region of cylinder members forming the biplane grid. However, the flow structure around square biplane grid is hardly known. Therefore, the aim of this study is to clarify the three-dimensional flow field around the circular cylinder members forming the square biplane grid by means of the measurement of surface pressure, the estimation of local drag coefficients and the flow visualization.

2. Experimental Apparatus and Methods

Figure 1 shows the coordinate system and nomenclature. The biplane grid, composed of circular cylinders with diameters of 10 mm, was used for the pressure measurement and flow visualization. The spacing ratio of the cylinders in each row is $L/d = 4$, where L is distance between adjacent cylinders and d is diameter of circular cylinder.

The wind tunnel with a cross section of 200 mm \times 200 mm was used for the measurement of the surface pressure on the cylinders. The biplane grid was placed in the position of 100 mm from the wind tunnel outlet. The pressure tapping hole with a diameter of 0.3 mm was drilled in each central cylinder surface of the upstream cylinder array and the downstream cylinder array, and the surface pressure was measured by rotating the circular cylinder in intervals of 5° from 0° to 180°. The Reynolds number was $Re = U_\infty \cdot d/\nu = 6000$, where U_∞ is free stream velocity approaching the biplane grid, and ν is kinematic viscosity of the air. The turbulence intensity is 0.6% for the free stream velocity. In order to

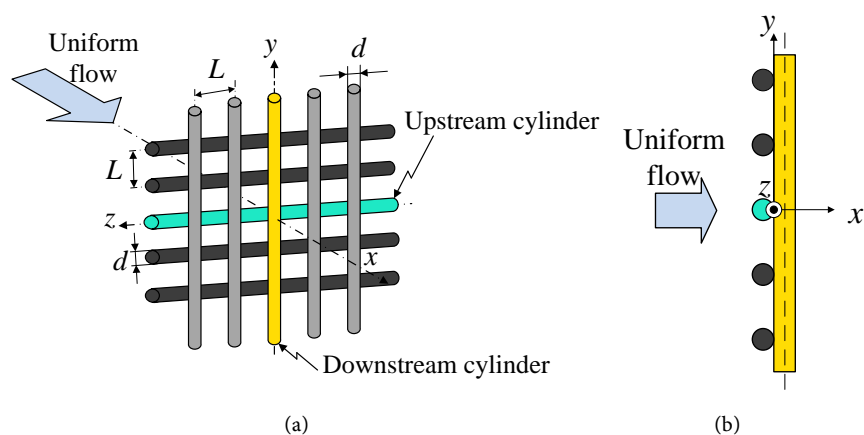


Figure 1. Coordinate system and nomenclature. (a) Biplane grid model; (b) Side view of Biplane grid.

measure the surface pressure on the cylinders, a minute differential pressure transducer was used. The sampling frequency was 1000 Hz, and the number of sampling was 10,000 points. The uncertainty of the pressure coefficient C_p was estimated to be approximately 5.5%.

Flow visualization was carried out in a water tunnel which has a cross-section of 400 mm × 400 mm. To take a picture of path lines, nylon particles with an average particle diameter of 50 μm and a specific gravity of 1.03 were mixed into the water flow. The experimental Reynolds number was kept to 200 for flow visualization. The measurement plane was $x/d = 2.0$.

3. Experimental Results and Discussions

3.1. Surface Pressure Distribution

Figure 2 shows the circumferential distributions of surface pressure coefficient C_p on the upstream and downstream cylinders of biplane grid. The surface pressure coefficient is defined as following equation, which P_∞ is the atmospheric pressure and ρ is the density of the air.

$$C_p = \frac{P - P_\infty}{(1/2)\rho U_\infty^2} \tag{1}$$

Figure 2 also shows the pressure distribution on the crossed circular cylinders ($Re = 2 \times 10^4$) by Fox *et al.* [10], the crossed circular cylinders ($Re = 4000$) by Yamada *et al.* [8], and the single cylinder ($Re = 6000$) for reference. In **Figure 2(a)**, the value of C_p in the range of approximately $130^\circ \leq \theta \leq 175^\circ$ at $z/d = 0$ symmetrical plane became significantly larger. At the other measurement planes, as the measurement plane of the upstream cylinder approaches $z/d = 0$ symmetrical plane, the pressure on the rear side rapidly increased. The increase in pressure may be caused by the high-speed flow which penetrates into the rear of the upstream cylinder beyond the separation bubble which is on the upstream cylinder surface [8] [9]. On the other hand, as shown in **Figure 2(b)**, the pressure distribution on the downstream cylinder are almost similar to one another,

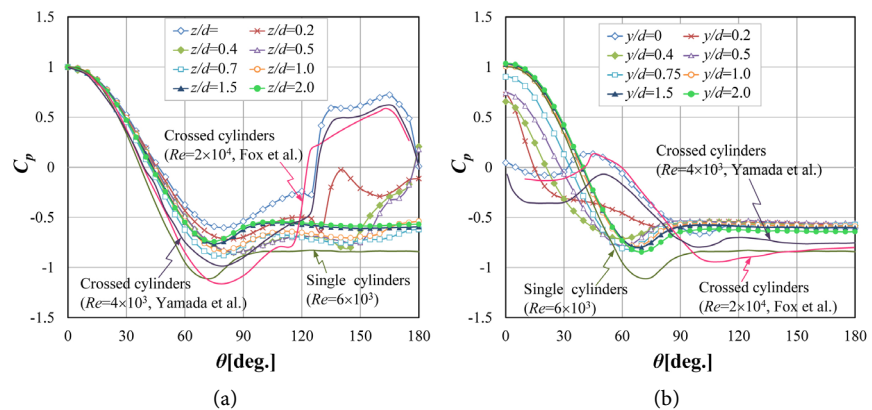


Figure 2. Surface pressure distributions. (a) At each z/d position along z -axis of upstream cylinder; (b) At each y/d position along y -axis of downstream cylinder.

excluding the case of $y/d = 0$ and $y/d = 0.2$ planes. In particular, in the case of $y/d = 0$, C_p took the maximum value at approximately $\theta = 45^\circ$, and the pressure gradient is negative in the range of $\theta \geq 45^\circ$. This phenomenon suggests that there is no separation in circumferential direction on the downstream cylinder, or the separation point on the downstream cylinder moves considerably backward in the vicinity of $y/d = 0$ symmetrical plane.

Figure 3 shows the spanwise distribution of the base pressure coefficient C_{pb} behind the upstream cylinder ($\theta = 180^\circ$), the spanwise distribution of the front pressure coefficient C_{p0} on the downstream cylinder ($\theta = 0^\circ$) and the spanwise distribution of the base pressure coefficient C_{pb} behind the downstream cylinder ($\theta = 180^\circ$). **Figure 3** also shows the results of the upstream and downstream cylinders in crossed circular cylinders ($Re = 4000$) by Yamada *et al.* [8]. As shown in **Figure 3(a)**, the base pressure distribution had the minimum value at $z/d = 0.2$, and then the maximum value at $z/d = 0.4$. The front pressure distribution in **Figure 3(b)** had the maximum value at approximately $y/d = 0.2$ and the minimum value at approximately $y/d = 0.4$. After that, it rose to approach a constant value. These distributions in **Figure 3(a)** and **Figure 3(b)** are similar to those of the crossed circular cylinders (Yamada *et al.* [8]). Yamada *et al.* reported the presence of the secondary-flow along spanwise and circumference on the surface of the upstream and downstream cylinders in the contact region by means of

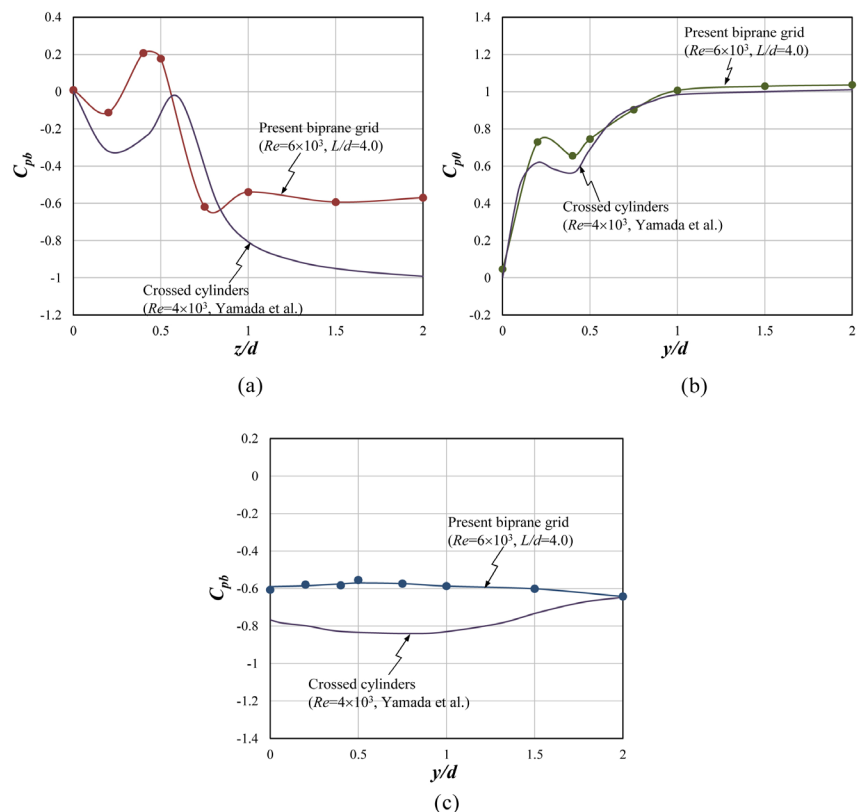


Figure 3. Spanwise pressure coefficient. (a) Upstream cylinder ($\theta = 180^\circ$); (b) Downstream cylinder ($\theta = 0^\circ$); (c) Downstream cylinder ($\theta = 180^\circ$).

oil-film methods. From this, it is suspected that there is a secondary-flow in the vicinity of the contact point between the upstream cylinder and the downstream cylinder of the biplane grid. Moreover, as shown in **Figure 3(c)**, the value of the base pressure on the downstream cylinder had an almost constant value at every measurement position.

3.2. Estimation of Local Drag Coefficient

Figure 4 shows the relationship between the local drag coefficient C_d on the upstream and downstream cylinders and the measurement position in each span. **Figure 4** also shows that of the upstream and downstream cylinders in the crossed circular cylinders ($Re = 4000$) by Yamada *et al.* [8] as well as the single cylinder ($Re = 6000$) for reference. The local drag coefficient C_d is defined as

$$C_d = \int_0^\pi C_p(\theta) \cos(\theta) d\theta. \quad (2)$$

In the case of the upstream cylinders, the value of C_d was rapidly increasing in the range from $z/d = 0$ to $z/d = 0.75$ and then gently decreasing in the range from $z/d = 0.75$ to $z/d = 2.0$. The former is understood as the influence of the high-speed flow which penetrates behind the upstream cylinder, as mentioned in **Figure 2(a)**. In the case of the downstream cylinder, the value of C_d decreased in the range from $y/d = 0$ to $y/d = 0.4$, the value of C_d in the region of $y/d \geq 1.0$ was almost constant. The tendency of the distribution is similar to that of the crossed circular cylinders. The value of C_d is thought to be smaller in the range of $0 \leq y/d \leq 0.4$, since there is no separation point or the separation point moves back, as mentioned in **Figure 2(b)**. In addition, both the value of C_d on the upstream cylinder and the downstream cylinder is lower than the value of C_d on the single cylinder.

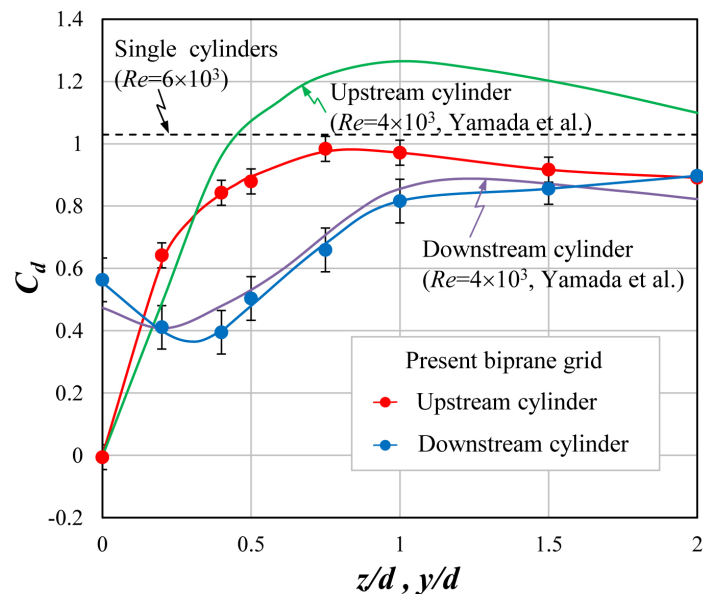


Figure 4. Local pressure drag coefficient.

3.3. Flow Visualization

Figure 5(a) and **Figure 6(a)** show the path lines pattern behind the biplane grid. **Figure 5(b)** and **Figure 6(b)** show the sketch of the flow pattern, which were drawn from the path lines movie behind the biplane grid. This path lines pattern varied with a cycle of approximately 25 seconds.

As shown in **Figure 5(a)** and **Figure 6(a)**, the secondary-flow was observed. In addition, the secondary-flow generates vortices which might be longitudinal vortices. In **Figure 5**, it was observed that two pairs of the vortices A' and B were formed in the range of about $y/d \leq \pm 1.0$ and $z/d \leq \pm 0.5$ behind the downstream cylinder, and B was rather small in comparison with A'. The flow around B was entrained into the A'. At the same time, the scale of the vortex pair A in the range of $3.0 \leq y/d \leq 4.0$ became larger. Similarly, as shown in **Figure 6**, the scale of vortex pair A' was smaller, the scale of vortex pair B became larger. At the same time, the scale of vortex pair B' in the range of $-4.0 \leq y/d \leq -3.0$ became larger. Based on the path lines movie observation, the scale of the vortex pairs (A, A') and (B, B') were alternately and periodically varied. The direction of the

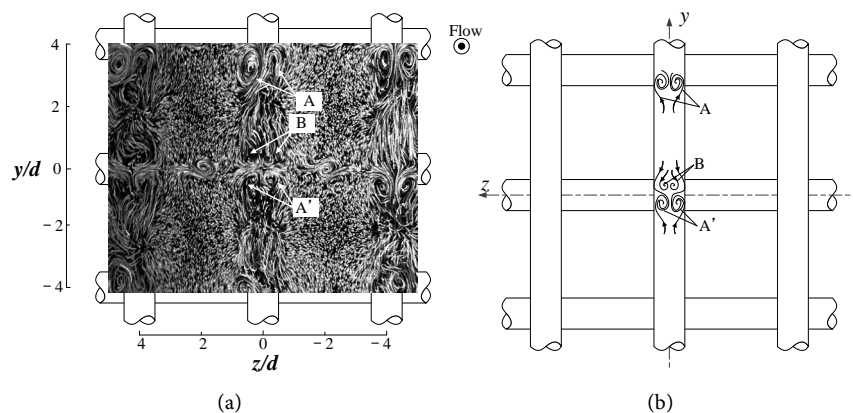


Figure 5. Flow visualization behind biplane grid (Vortices A, A' became larger). (a) Path lines pattern; (b) Sketch of flow pattern.

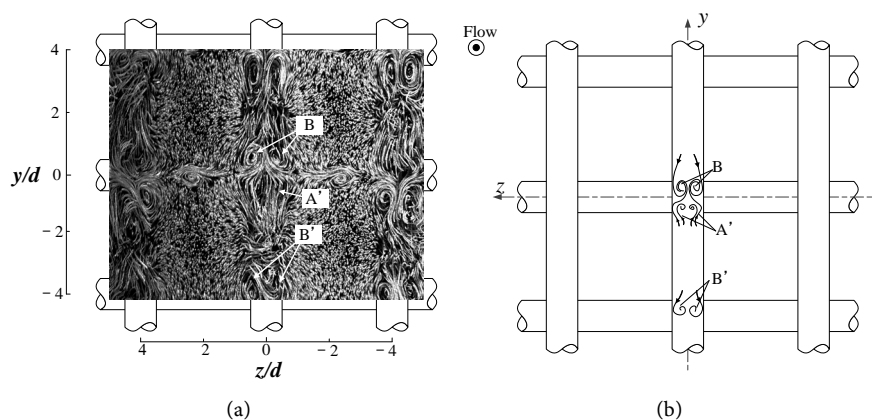


Figure 6. Flow visualization behind biplane grid (Vortices B, B' became larger). (a) Path lines pattern; (b) Sketch of flow pattern.

flow which moved backward on $y/d = 0$ symmetrical plane on the surface of the downstream cylinder corresponds to the rotation direction of the vortices.

4. Conclusion

The characteristics of the three-dimensional flow field around the circular cylinder members forming the square biplane grid were investigated by the measurement of surface pressure, the estimation of the local drag coefficient and the flow visualization of path lines. As a result, it was found that the drag coefficient of circular cylinders forming a biplane grid was much reduced compared to that of the single cylinder. A drag reduction would be caused by the secondary-flow.

References

- [1] Sakai, Y., Nagata, K., Suzuki, H. and Ito, Y. (2016) Mixing and Diffusion in Regular/Fractal Grid Turbulence. In: Sakai, Y. and Vassilicos, C., Eds., *Fractal Flow Design: How to Design Bespoke Turbulence Why*, Springer, 17-73.
- [2] Shiozaki, T., Maruyama, S., Mohri, T. and Hozumi, Y. (2005) Fluid Flow Characteristics through a Wire Mesh at Low Reynolds Number for High Temperature Air Combustion Furnace. *Transactions of the Japan Society of Mechanical Engineers B*, **71**, 163-166. (In Japanese)
- [3] Antonia, R.A., Zhou, T. and Zhu, Y. (1998) Three-Component Vorticity Measurements in a Turbulent Grid Flow. *Journal of Fluid Mechanics*, **374**, 29-57. <https://doi.org/10.1017/S0022112098002547>
- [4] Zhou, T. and Antonia, R.A. (2000) Reynolds Number Dependence of the Small-Scale of Grid Turbulence. *Journal of Fluid Mechanics*, **406**, 81-107. <https://doi.org/10.1017/S0022112099007296>
- [5] Livescu, D., Jaber, F.A. and Madnia, C.K. (2000) Passive-Scalar Wake behind a Line Source in Grid Turbulence. *Journal of Fluid Mechanics*, **416**, 117-149. <https://doi.org/10.1017/S0022112000008910>
- [6] Mydlarski, L. and Warhaft, Z. (1998) Passive Scalar Statistics in High-Peclet-Number Grid Turbulence, *Journal of Fluid Mechanics*, **358**, 135-175. <https://doi.org/10.1017/S0022112097008161>
- [7] de Bray, B.G. (1967) Some Investigation into the Spanwise Non-Uniformity of Normally Two-Dimensional Incompressible Boundary Layers Downstream of Gauze Screens. *Aeronautical Research Council Reports and Memoranda*, **3578**, 1-18.
- [8] Yamada, H., Osaka, H., Kageyama, Y. and Takeda, O. (1987) The Flow around the Crossed Two Circular Cylinders Normal to the Uniform Stream. *Transactions of the Japan Society of Mechanical Engineers B*, **53**, 333-340. (In Japanese)
- [9] Yamada, H., Mizobe, R., Hayashi, E. and Iwamoto, M. (2011) Visualization of Vortices Pattern in the Interval Space between Two Separately Crossed Circular Cylinders. *Proceedings of the 11th Asian Symposium on Visualization*, Niigata, 5-9 June 2011, 11.
- [10] Fox, T.A. and Toy, N. (1988) Fluid Flow at the Center of a Cross Composed of Tubes. *International Journal of Heat and Fluid Flow*, **9**, 53-61. [https://doi.org/10.1016/0142-727X\(88\)90030-6](https://doi.org/10.1016/0142-727X(88)90030-6)

Nomenclature

- x, y, z : Cartesian coordinate system
 d : Diameter of circular cylinder
 L : Distance between adjacent cylinders
 θ : Circumference degree of circular cylinder
 U_∞ : Free stream velocity approaching biplane grid
 P : Surface pressure on circular cylinder
 P_∞ : Atmospheric pressure
 ν : Kinematic viscosity
 ρ : Density of air
 Re : Experimental Reynolds number
 C_p : Surface pressure coefficient
 C_{p0} : Front pressure coefficient
 C_{pb} : Base pressure coefficient
 C_d : Local pressure drag coefficient